Proceedings of the 45th IEEE Conference on Decision & Control
Manchester Grand Hyatt Hotel
San Diego, CA, USA, December 13-15, 2006

Time-Varying Angular Rate Sensing for a MEMS Z-Axis Gyroscope[1]

Mohammad Salah†, Michael McIntyre†, Darren Dawson†, and John Wagner‡
†Department of Electrical & Computer Engineering, Clemson University, Clemson, SC 29634
‡Department of Mechanical Engineering, Clemson University, Clemson, SC 29634
E-mail: msalah@ces.clemson.edu

Abstract: In this paper, both axes of a z-axis MEMS gyroscope are actively controlled to facilitate time-varying angular rate sensing. An off-line adaptive least-squares estimation strategy is first developed that accurately estimates the unknown model parameters. An estimation analysis is presented which proves that the model parameters are accurately estimated. An on-line active controller/observer is then developed for time-varying angular rate sensing. For this method, a nonlinear estimator is developed based on a Lyapunov-based analysis, which proves that the time-varying angular rate experienced by the device can be estimated accurately.

1 Introduction

Gyroscopes are often used to measure the angular rate in many navigation, homing, and stabilization applications. Recently, the development of microelectromechanical (MEMS) gyroscopes ([1], [5], [14], and [15]) have increased the range of applications for these devices. The advantage of MEMS gyroscopes over conventional inertial navigation instruments include [5], and [6]: 1) compact size, 2) decreased weight, 3) low power consumption, 4) low cost micromachining process, and 5) ease of mass production. These factors offer a wide range of applications for MEMS gyroscopes [16], ranging from stability and navigation control in spacecraft, rollover detection for automotive applications, consumer electronics, robotics, and a variety of military applications.

Practically all MEMS gyroscopes provide angular rate measurements using vibrational elements; hence, these devices are referred to as vibrational gyroscopes. Previous research has implemented a *drive axis/sense axis* methodology for angular rate sensing [3], [7], and [13]. Using this method, the gyroscope consists of a mass suspended on elastic flexures anchored to the substrate of the device. This mass is driven at its resonate frequency and the rotation induced Coriolis force generates the transfer of energy from the drive vibrational plane to the sense vibrational plane: these are the x-y plane in case of the z-axis gyroscope [1]. For MEMS gyroscopes to realize the performance levels of which they are capable, innovative methods are required for device calibration, accurate model identification, and active control of sensor dynamics for angular rate sensing ([5], [6], and [13]).

Past MEMS gyroscope research has focused on the development of the microelectromechanical fabrication processes ([1], [14], and [15]), sensor modeling ([5], [6], and [12]), and the active control of the sensor dynamics for model identification and angular rate sensing ([3], [6], [8], and [13]). In [5], M'Closkey *et al.* present a dynamic model for the *JPL microgyro.* This work is extended in [6], where the authors presented a recursive least-squares algorithm to identify the parameters of the physical model using available sensor information. In [12], Shkel *et al.* present both adaptive and non-adaptive nonlinear methods for the active control of the sensor dynamics for angular rate sensing. The approach presented in [12] aims to compensate the model inaccuracies under the assumption that the angular rate is constant. In [3], Leland developed an adaptive controller to tune the drive vibrational plane's resonant frequency, which is not known *a priori,* to provide angular rate sensing; however this method assumes a constant angular rate. The authors of [8] and [9] present a linear adaptive operation strategy for MEMS z-axis gyroscopes under the assumption of a constant angular rate. This work deviates from the traditional *drive axis/sense axis* methodology due to a lack of meeting the persistence of excitation condition that is required for compensation of the fabrication defects and perturbations affecting the behavior of a MEMS z-axis gyroscope. Other research has been presented that develops alternate drive method, similar to the results of [8] and [9] that drive both axes of the z-axis MEMS gyroscope. In [2], the authors extended the previous development of [3] to develop controllers for both axes. The work in [2] utilizes an adaptive resonant frequency tuning controller for the drive axis and develops an adaptive controller for angular rate sensing, under the

[1]This research was supported in part by two DOC Grants, an ARO Automotive Center Grant, a DOE Contract, a Honda Corporation Grant, and a DARPA Contract.

assumption that the time-varying angular rate can be approximated by a polynomial function in a finite time interval.

In this paper, both axes of the device are actively controlled to develop a strategy for estimating the time-varying angular rate for a z-axis MEMS gyroscope. An off-line parameter estimation strategy is first developed that places the gyroscope in a condition of zero angular rate. A reference input is used to excite both axes such that a subsequently required *persistence of excitation* condition is met. Standard adaptive least-squares estimator is utilized to estimate the unknown model parameters. An analysis is presented which proves that these parameters are accurately estimated. Based on exact knowledge of the model parameters, an on-line active controller/observer is then developed for time-varying angular rate sensing. For this method, a nonlinear algorithm is developed based on a Lyapunov-based analysis, which proves that the time-varying angular rate experienced by the device is estimated accurately.

This paper is organized as follows. In Section 2, the dynamic system model for a MEMS gyroscope is defined, along with the required assumptions for this analysis. In Section 3, the adaptive least-squares estimator is presented along with the analysis which verifies that under a set of sufficient conditions in which the model parameters are accurately estimated. In Section 4, a nonlinear algorithm is developed along with an analysis which verifies that under a set of sufficient conditions the time-varying angular rate is accurately estimated. Concluding remarks are provided in Section 5.

2 System Dynamics and Assumptions

A z-axis, non-ideal MEMS gyroscope is depicted in Figure 1. From the diagram shown in Figure 1, the dynamic model can be written in the Cartesian coordinate system as follows [12]

$$M\ddot{q} + D\dot{q} + Kq = \tau + S\dot{q} \tag{1}$$

where $q(t) \triangleq [x(t), y(t)]^T \in \mathbb{R}^2$ is the displacement of the gyroscope's reference point, and $x(t), y(t) \in \mathbb{R}$. In (1) $\dot{q}(t), \ddot{q}(t) \in \mathbb{R}^2$ are the velocity and acceleration of the gyroscope's reference point, respectively, $M \in \mathbb{R}^{2\times 2}$ denotes the inertia effect, $D \in \mathbb{R}^{2\times 2}$ denotes the damping ratio, $K \in \mathbb{R}^{2\times 2}$ denotes the spring constant, $S(t) \in \mathbb{R}^{2\times 2}$ denotes the centripetal-Coriolis effect, and $\tau(t) \triangleq [\tau_x(t), \tau_y(t)]^T \in \mathbb{R}^2$ is the control input, where $\tau_x(t), \tau_x(t) \in \mathbb{R}$. The terms M and $S(t)$ can be expanded as follows [12]

$$M = \begin{bmatrix} m & 0 \\ 0 & m \end{bmatrix}, S = \begin{bmatrix} 0 & 2m\Omega_z \\ -2m\Omega_z & 0 \end{bmatrix} \tag{2}$$

where $m \in \mathbb{R}$ is the reference point's mass within the gyroscope, and $\Omega_z(t) \in \mathbb{R}$ is the angular rate about the z-axis. The angular rates $\Omega_x(t)$ and $\Omega_y(t)$ around the x and y axes, respectively, are assumed to be zero.

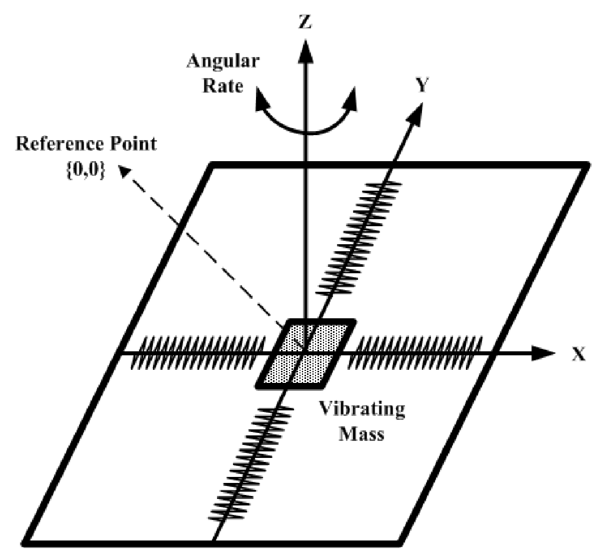

Figure 1: Simple mass-spring model of z-axis gyroscope

Because of the presence of imperfections in the fabrication process, D and K can be expanded as follows [12]

$$D = \begin{bmatrix} d_{xx} & d_{xy} \\ d_{yx} & d_{yy} \end{bmatrix}, K = \begin{bmatrix} k_{xx} & k_{xy} \\ k_{yx} & k_{yy} \end{bmatrix} \tag{3}$$

where $d_{xx}, d_{yy} \in \mathbb{R}$ are the damping ratios along the x and y axes, respectively, $d_{xy}, d_{yx} \in \mathbb{R}$ are the damping ratios affecting both x and y axes, $k_{xx}, k_{yy} \in \mathbb{R}$ are the spring constants along the x and y axes, respectively, $k_{xy}, k_{yx} \in \mathbb{R}$ are the spring constants affecting both x and y axes. In order to facilitate the off-line parameter and on-line angular rate estimation strategies, the following assumptions frame the analysis.

Assumption 1: The gyroscope's parameters $m, d_{xx}, d_{yy}, k_{xx}$ and k_{yy} are unknown and assumed to be constants with respect to time.

Assumption 2: The damping ratios d_{xy} and d_{yx}, and the stiffness k_{xy} and k_{yx} are equal to zero, precedence for this assumption can be found in [3] and [8]. It should be noted that the subsequent development could be extended such that these parameters could also be estimated.

Assumption 3: The angular rate and its first two time derivatives are bounded, which means $\Omega_z(t), \dot{\Omega}_z(t), \ddot{\Omega}_z(t) \in L_\infty$, hence, it is clear that

$S(t), \dot{S}(t), \ddot{S}(t)$ are upper bounded as follows

$$\|S(t)\| \le \Gamma_1 \qquad \left\|\dot{S}(t)\right\| \le \Gamma_2 \qquad \left\|\ddot{S}(t)\right\| \le \Gamma_3 \tag{4}$$

where $\Gamma_1, \Gamma_2, \Gamma_3 \in \mathbb{R}^+$ are bounding constants.

3 Off-Line Parameter Estimation

For the development of an off-line parameter estimation strategy, the system is configured such that the angular rate is equal to zero (*i.e.*, $\Omega_z(t) = 0$). The following assumption is required so that a reference input is injected at $\tau(t)$ in (1) such that $q(t), \dot{q}(t)$ and $\ddot{q}(t)$ are bounded.

Assumption 4: The reference input $\tau(t)$ is designed to be a bounded, piecewise continuous function.

The dynamic model in (1) can then be rewritten as follows

$$M\ddot{q} + D\dot{q} + Kq = \tau. \tag{5}$$

Due to the fact that $\ddot{q}(t)$ is unmeasurable, a torque filtering technique [4] is used for this development. The dynamic model in (5) can be written as follows

$$\tau = \dot{h} + g \tag{6}$$

where $h(t), g(t) \in \mathbb{R}^2$ are defined as follows

$$\dot{h} \triangleq \frac{d}{dt}(M\dot{q}) = M\ddot{q} \qquad g \triangleq D\dot{q} + Kq. \tag{7}$$

To facilitate the off-line parameter estimator design, a filtered torque signal $\tau_f(t) \in \mathbb{R}^2$ can be defined as follows

$$\tau_f \triangleq f * \tau \tag{8}$$

where $(*)$ is the convolution operator, and $f(t) \in \mathbb{R}$ is the impulse response of a linear stable, strictly proper filter and can be defined as a first-order filter as follows

$$f \triangleq \alpha e^{-\beta t} \tag{9}$$

where $\alpha, \beta \in \mathbb{R}^+$are constants. After substituting (6) into (8), the following expression can be obtained utilizing standard convolution properties

$$\begin{aligned} \tau_f &= f * \dot{h} + f * g \\ &= \dot{f} * h + f_o h - f h_o + f * g \end{aligned} \tag{10}$$

where f_o and h_o denote that $f(t)$ and $h(t)$ are computed at the initial time t_o. To facilitate the design of the off-line parameter estimator, the expression in (8) can be written in terms of the following linear parameterization

$$\tau_f = W_f \theta \tag{11}$$

where $\theta \in \mathbb{R}^5$ is a vector of the unknown constant parameters, and $W_f(q, \dot{q}) \in \mathbb{R}^{2\times 5}$ is the known filtered regression matrix, where θ and $W_f(q, \dot{q})$ are defined as follows

$$\begin{aligned} \theta &\triangleq \begin{bmatrix} m & d_{xx} & k_{xx} & d_{yy} & k_{yy} \end{bmatrix}^T \\ W_f &\triangleq \begin{bmatrix} W_{f11} & W_{f12} & W_{f13} & 0 & 0 \\ W_{f21} & 0 & 0 & W_{f24} & W_{f25} \end{bmatrix}. \end{aligned} \tag{12}$$

The elements of the regression matrix are generated using the following expressions

$$\begin{aligned} W_{f11} &= \alpha\dot{x} + p_x + \alpha e^{-\beta t_o}\dot{x} - \alpha e^{-\beta t}\dot{x}_o \\ \dot{W}_{f12} &= -\beta W_{f12} + \alpha\dot{x} \\ \dot{W}_{f13} &= -\beta W_{f13} + \alpha x \\ W_{f21} &= \alpha\dot{y} + p_y + \alpha e^{-\beta t_o}\dot{y} - \alpha e^{-\beta t}\dot{y}_o \\ \dot{W}_{f24} &= -\beta W_{f24} + \alpha\dot{y} \\ \dot{W}_{f25} &= -\beta W_{f25} + \alpha y \end{aligned} \tag{13}$$

where α and β were introduced in (9), $W_{f11}(t), W_{f12}(t), W_{f13}(t), W_{f21}(t), W_{f24}(t), W_{f25}(t) \in \mathbb{R}$, $\dot{x}_o$ and $\dot{y}_o$ denote that $\dot{x}(t)$ and $\dot{y}(t)$ are computed at the initial time t_o, and $p_x(t), p_y(t) \in \mathbb{R}$ are auxiliary filter signals, and defined as follows

$$\begin{aligned} \dot{p}_x &= -\beta p_x - \alpha\beta\dot{x} \\ \dot{p}_y &= -\beta p_y - \alpha\beta\dot{y}. \end{aligned} \tag{14}$$

Furthermore, $W_{f12}(t_o) = W_{f13}(t_o) = W_{f24}(t_o) = W_{f25}(t_o) = p_x(t_o) = p_y(t_o) = 0$. Since θ is a vector of uncertain parameters, the structure of (11) cannot be implemented. An implementable form (i.e., a measurable and acceleration independent form) of (11) can be determined by utilizing (8) and (9) to generate the filtered torque signal via the following differential equation

$$\dot{\tau}_f = -\beta\tau_f + \alpha\tau \qquad \tau_f(t_o) = \emptyset_2 \tag{15}$$

where $\emptyset_2 \in \mathbb{R}^2 = [0, 0]^T$ is a vector of zeros.

Lemma 1 *The parametrized model described by (11)-(14) is equal to the filtered torque dynamics described by (15).*

Proof: See Appendix 1 in [10].

Let the estimate of the filtered torque $\widehat{\tau}_f(t) \in \mathbb{R}^2$ be defined as follows

$$\hat{\tau}_f \triangleq W_f\widehat{\theta} \tag{16}$$

where $\widehat{\theta}(t) \in \mathbb{R}^5$ is the estimate of the unknown parameters, and $W_f(\dot{q}, q)$ is defined in (12)-(14). An error signal $\varepsilon(t) \in \mathbb{R}^2$ can also be defined as follows

$$\varepsilon \triangleq \tau_f - \hat{\tau}_f = W_f\widetilde{\theta} \tag{17}$$

where the parameter estimate error $\widetilde{\theta}(t) \in \mathbb{R}^5$ is defined as follows

$$\widetilde{\theta} \triangleq \theta - \widehat{\theta}. \tag{18}$$

The following adaptive update rule can be generated using the least-squares estimation method as follows [4]

$$\dot{\hat{\theta}} \triangleq kPW_f^T\varepsilon \tag{19}$$

where $k \in \mathbb{R}^+$ is a constant, and $P(t) \in \mathbb{R}^{5\times5}$ is the covariance matrix. This matrix $P(t)$ is generated by the covariance propagation equation, which is described as follows [4]

$$\dot{P} \triangleq -kPW_f^TW_fP \tag{20}$$

Theorem 1 *The least-squares estimation strategy as described in (19) and (20) ensures that $\widetilde{\theta}(t) \to 0$ as $t \to \infty$ provided the following sufficient conditions are met: (i) the plant of estimation is strictly proper, (ii) the input is piecewise continuous and bounded, (iii) the output of the plant of estimation is bounded, and the following persistence of excitation condition [11] holds*

$$\gamma_1 I_5 \leqslant \int_t^{t+\delta} W_f^T(\sigma)W_f(\sigma)d\sigma \leqslant \gamma_2 I_5 \tag{21}$$

where $\gamma_1, \gamma_2, \delta \in \mathbb{R}^+$ are constants, $I_5 \in \mathbb{R}^{5\times5}$ is the identity matrix, and $W_f(.)$ is defined by (12)-(14).

Proof: To prove that $\widetilde{\theta}(t) \to 0$ as $t \to \infty$, Theorem 2.5.3 from [11] is followed directly. To prove that sufficient condition (i) is valid; it is clear that the plant of estimation described in (15) is strictly proper. To prove that sufficient condition (ii) is valid; the reference input (*i.e.* $\tau(t)$) to the plant is designed such that it is piecewise continuous and bounded. To prove that sufficient condition (iii) is valid; it is clear that since $\tau(t)$ has been designed to be bounded, then from standard linear analysis tools, (15) can be used to show that $\tau_f(t), \dot{\tau}_f(t) \in \mathcal{L}_\infty$.

4 On-Line Angular Rate Estimator Design

For the on-line time-varying angular rate estimator development, the subsequent analysis will prove a global asymptotic result provided that the displacement $q(t)$ and velocity $\dot{q}(t)$ of the gyroscope's reference point are measurable and that model parameters as defined in (12) are known *a priori*. This development requires that the control input $\tau(t)$, introduced in (1), is designed to force $q(t)$ to track a desired trajectory $q_d(t) \triangleq [x_d(t), y_d(t)]^T \in \mathbb{R}^2$, where $x_d(t), y_d(t) \in \mathbb{R}$, to facilitate the estimation of the time-varying angular rate $\Omega_z(t)$. This also requires that the desired trajectory and its first three time derivatives are bounded, hence, it is assumed that $q_d(t), \dot{q}_d(t), \ddot{q}_d(t), \dddot{q}_d\,(t) \in L_\infty$.

4.1 Estimator Design Objectives

The control objective of the angular rate estimator is to ensure that the reference point's displacement $q(t)$ tracks the desired trajectory $q_d(t)$ in the following sense

$$q(t) \to q_d(t) \quad as \quad t \to \infty. \tag{22}$$

The estimator objective is to ensure that the estimated angular rate, denoted by $\widehat{\Omega}_z(t) \in \mathbb{R}$, converges to the actual rate in the following sense

$$\widehat{\Omega}_z(t) \to \widehat{\Omega}_z(t) \quad as \quad t \to \infty. \tag{23}$$

To facilitate the subsequent development and analysis, the control objective is achieved through a filtered tracking error signal, denoted by $r(t) \in \mathbb{R}^2$, that is defined as follows

$$r \triangleq \dot{e}_2 + \alpha_2 e_2 \tag{24}$$

where $e_2(t) \in \mathbb{R}^2$ is defined as follows

$$e_2 \triangleq \dot{e}_1 + \alpha_1 e_1 \tag{25}$$

where $\alpha_1, \alpha_2 \in \mathbb{R}^+$ are control gains, and $e_1(t) \in \mathbb{R}^2$ is defined as follows

$$e_1 \triangleq q_d - q. \tag{26}$$

Based on the definition of $e_1(t)$ in (26), it is clear that if $e_1(t) \to 0 \quad as \quad t \to \infty$ then $q(t) \to q_d(t) \quad as \quad t \to \infty$, thus, meeting the control objective.

4.2 Closed-Loop Error System

To facilitate the development of the closed-loop error system for $r(t)$, the error system dynamics for $e_1(t)$ and $e_2(t)$ are first examined. To this end, the second time derivative of (26) is taken and then both sides are multiplied by M, thus, obtaining the following expression

$$M\ddot{e}_1 = M\ddot{q}_d + D\dot{q} + Kq - S\dot{q} - \tau \tag{27}$$

where (1) was utilized. The control input $\tau(t)$ is designed as follows

$$\tau \triangleq M\ddot{q}_d + D\dot{q} + Kq - \widehat{F} \tag{28}$$

where $\hat{F}(t) \in \mathbb{R}^2$ is an auxiliary signal to be subsequently designed. After substituting (28) into (27), the following expression can be obtained

$$M\ddot{e}_1 = \widehat{F} - S\dot{q}. \tag{29}$$

From the definition in (25) and utilizing the time derivative of (29), the following expression can be obtained

$$M\ddot{e}_2 = \dot{\widehat{F}} - \dot{S}\dot{q} - S\ddot{q} + \alpha_1 M\ddot{e}_1. \tag{30}$$

The closed-loop error system dynamics now can be written as follows

$$M\dot{r} = \dot{\widehat{F}} - \dot{S}\dot{q} - S\ddot{q} + \alpha_1 M\ddot{e}_1 + \alpha_2 M\dot{e}_2 \tag{31}$$

where (24) was pre-multiplied by M, and (30) was utilized. To facilitate the subsequent analysis, the expression in (31) is rewritten as follows

$$M\dot{r} = \tilde{N} + N_d + \dot{\widehat{F}} - e_2 \qquad (32)$$

where the auxiliary signal $\tilde{N}(q, \dot{q}, \ddot{q}, t) \in \mathbb{R}^2$ is defined as follows

$$\tilde{N} \triangleq N - N_d \qquad (33)$$

where $N(q, \dot{q}, \ddot{q}, t) \in \mathbb{R}^2$ is defined as follows

$$N \triangleq -\dot{S}\dot{q} - S\ddot{q} + \alpha_1 M\ddot{e}_1 + \alpha_2 M\dot{e}_2 + e_2 \qquad (34)$$

and $N_d(t) \in \mathbb{R}^2$ is defined as follows

$$\begin{aligned} N_d &\triangleq N|_{q=q_d, \dot{q}=\dot{q}_d, \ddot{q}=\ddot{q}_d} \\ &= -\dot{S}\dot{q}_d - S\ddot{q}_d. \end{aligned} \qquad (35)$$

Based on (32), the auxiliary signal $\widehat{F}(t)$, introduced in (28), is designed as follows

$$\begin{aligned} \widehat{F} &= -(k_s + 1)\left[e_2(t) - e_2(t_o) + \alpha_2 \int_{t_o}^{t} e_2(\sigma)d\sigma\right] \\ &\quad -\beta_1 \int_{t_o}^{t} sgn\left(e_2(\sigma)\right)d\sigma \end{aligned} \qquad (36)$$

where $k_s, \beta_1 \in \mathbb{R}^+$ are control gains, t_o is the initial time, and $sgn(.) \in \mathbb{R}^2$ denotes the vector signum function. The term $e_2(t_o)$ in (36) is included so that $\widehat{F}(t_o) = \emptyset_2$, where $\emptyset_2$ was introduced in (15). The time derivative of (36) is given by the following expression

$$\dot{\widehat{F}} = -(k_s + 1)r - \beta_1 sgn(e_2). \qquad (37)$$

After substituting (37) into (32), the following closed-loop error system can be obtained

$$M\dot{r} = \tilde{N} + N_d - (k_s + 1)r - \beta_1 sgn(e_2) - e_2. \qquad (38)$$

Remark 1 *Based on the expression in (35), and the fact that $q_d(t), \dot{q}_d(t), \ddot{q}_d(t), \dddot{q}_d(t) \in L_\infty$, then $\|N_d(t)\|$ and $\left\|\dot{N}_d(t)\right\|$ can be upper bounded by known positive constants $\varsigma_1, \varsigma_2 \in \mathbb{R}$ as follows*

$$\|N_d\| \leq \varsigma_1 \qquad \left\|\dot{N}_d\right\| \leq \varsigma_2. \qquad (39)$$

4.3 Stability Analysis

Theorem 2 *The controller given in (28) and (36), ensures that $e_1(t), \dot{e}_1(t), \ddot{e}_1(t) \to 0$ as $t \to \infty$ and all closed-loop signals are bounded provided the control gain β_1, introduced in (36), is selected to satisfy the following sufficient condition*

$$\beta_1 > \varsigma_1 + \frac{1}{\alpha_2}\varsigma_2 \qquad (40)$$

where ς_1 and ς_2 are given in (39), the control gains α_1 and α_2 are selected to be greater than 2, and k_s is selected sufficiently large.

Proof: See Appendix 2 in [10].

4.4 Estimation of $\Omega_z(t)$

The expression in (29) can be rewritten as follows

$$\widehat{F} - S\dot{q}_d = M\ddot{e}_1 - S\dot{e}_1 \qquad (41)$$

where the time derivative of (26) was utilized. Let the error signal $\tilde{F}(t) \in \mathbb{R}^2$ be defined as follows

$$\tilde{F} = \begin{bmatrix} \tilde{F}_1 \\ \tilde{F}_2 \end{bmatrix} = \begin{bmatrix} \widehat{F}_1 - F_1 \\ \widehat{F}_2 - F_2 \end{bmatrix} = M\ddot{e}_1 - S\dot{e}_1 \qquad (42)$$

where $F_1(t), F_2(t), \widehat{F}_1(t), \widehat{F}_2(t), \tilde{F}_1(t), \tilde{F}_2(t) \in \mathbb{R}$. From the proof of Theorem 2, it is clear that $e_1(t), \dot{e}_1(t), \ddot{e}_1(t) \to 0$ as $t \to \infty$, hence, $\tilde{F}(t) \to 0$ as $t \to \infty$, then $\widehat{F}(t) \to F(t)$ as $t \to \infty$, where the elements of $F(t)$ can be defined as follows

$$\begin{aligned} F_1 &\triangleq 2m\Omega_z\dot{y}_d \\ F_2 &\triangleq -2m\Omega_z\dot{x}_d. \end{aligned} \qquad (43)$$

Let the auxiliary function $\Delta(t) \in \mathbb{R}$ be defined as follows

$$\Delta \triangleq -\dot{x}_d F_2 + \dot{y}_d F_1 \qquad (44)$$

then the expression in (44) can be rewritten as follows

$$\Delta = 2m\Omega_z\left(\dot{x}_d^2 + \dot{y}_d^2\right) \qquad (45)$$

where (43) was utilized. From (44) and (45), an expression for the time-varying angular rate $\Omega_z(t)$ can be defined as follows

$$\Omega_z = \frac{\Delta}{2m\left(\dot{x}_d^2 + \dot{y}_d^2\right)} = \frac{\dot{y}_d F_1 - \dot{x}_d F_2}{2m\left(\dot{x}_d^2 + \dot{y}_d^2\right)}. \qquad (46)$$

Remark 2 *From (46), it is clear that special care needs to be taken to avoid $(\dot{x}_d^2(t) + \dot{y}_d^2(t)) = 0$. To avoid this condition, $\dot{x}_d(t)$ and $\dot{y}_d(t)$ must be designed such that $(\dot{x}_d^2(t) + \dot{y}_d^2(t))$ is never equal to zero.*

Based on the expression in (46), the estimated varying-time angular rate $\widehat{\Omega}_z(t) \in \mathbb{R}$ can be written as follows

$$\widehat{\Omega}_z = \frac{\dot{y}_d\widehat{F}_1 - \dot{x}_d\widehat{F}_2}{2m\left(\dot{x}_d^2 + \dot{y}_d^2\right)} \qquad (47)$$

where $\widehat{F}_1(t)$ and $\widehat{F}_2(t)$ are generated by (36). An angular rate error signal $\widetilde{\Omega}_z(t) \in \mathbb{R}$ can be calculated from (46) and (47) as follows

$$\widetilde{\Omega}_z \triangleq \widehat{\Omega}_z - \Omega_z = \frac{\dot{y}_d\widetilde{F}_1 - \dot{x}_d\widetilde{F}_2}{2m\left(\dot{x}_d^2 + \dot{y}_d^2\right)}. \qquad (48)$$

From (48), it is clear that since $\widetilde{F}_1(t), \widetilde{F}_2(t) \to 0$ as $t \to \infty$, then, $\widetilde{\Omega}_z(t) \to 0$ as $t \to \infty$, hence, $\widehat{\Omega}_z(t) \to \Omega_z(t)$.

5 Conclusion

This work developed an active controller/observer for a z-axis MEMS gyroscope where both axes are driven. An off-line adaptive least-squares estimation strategy and analysis were presented that proved if the system is persistently excited, then the parameters of the dynamic model can be estimated. An on-line time-varying angular rate sensing nonlinear algorithm that is based on a Lyapunov analysis is also presented. This on-line nonlinear algorithm requires that model parameters to be known *a priori*.

References

[1] W. A. Clark, R. T. Howe, and R. Horowitz, "Surface Micromachined Z-Axis Vibratory Rate Gyroscope," *Proc. IEEE Solid State Sensors and Actuators Workshop*, Hilton Head Island, SC, June 1996, pp 283-287.

[2] L. Dong, and R. P. Leland, "The Adaptive Control System of a MEMS Gyroscope with Time-Varying Rotation Rate," *Proc. of the American Control Conference*, Portland, OR, June 2005, vol. 5, pp. 3592 - 3597.

[3] R. P. Leland, "Adaptive Mode Tuning for Vibrational Gyroscopes," *IEEE Trans. on Control Systems Technology*, March 2003, vol. 11, no. 2, pp. 242-247.

[4] F. L. Lewis, D. M. Dawson, and C. T. Abdallah, "Robot Manipulator Control: Theory and Practice," 2nd edition, NY: Marcel Dekker, Inc., 2004.

[5] R. T. M'Closkey, S. Gibson, and J. Hui, "Model Parameter Identification of a MEMS Gyroscope," *Proc. of the American Control Conference*, Chicago, IL, June 2000, pp. 1699-1704.

[6] R. T. M'Closkey, J. S. Gibson, and H. J. Hui, "Input-Output Dynamics of the JPL Microgyroscope," *Proc. 37th IEEE Conf. Decision and Control*, Dec 1998, vol. 4, pp. 4328-4333.

[7] P.R. Pagilla, and Y. Zhu, "Adaptive Control of Mechanical Systems with Time-Varying Parameters and Disturbances," *Journal of Dynamic Systems, Measurement, and Control*, vol. 126, no. 3, pp. 520-530, Sep 2004.

[8] S. Park, and R. Horowitz, "Adaptive Control for the Conventinal Mode of Operation of MEMS Gyroscopes," *Journal of Microelectromechanical Systems*, vol. 12, no. 1, pp. 101-108, Feb 2003.

[9] S. Park, and R. Horowitz, "Adaptive Control for Z-Axis MEMS Gyroscopes," *Proc. American Control Conf.*, Arlington, VA, June 2001, vol. 2, pp. 1223-1228.

[10] M. Salah, M, McIntyre, D. M. Dawson, J. Wagner, "Time-Varying Angular Rate Sensing for a MEMS Z-Axis Gyroscope," Clemson University CRB Technical Report, CU/CRB/2/24/06/#1, http://www.ces.clemson.edu/ece/crb/publictn/tr.htm.

[11] S. Sastry, and M. Bodsom, "Adaptive Control: Stability, Convergence and Robustness," Englewood Cliffs, NJ: Prentice Hall, Inc., 1989.

[12] A. Shkel, R.T. Howe, and R. Horowitz, "Modeling and Simulation of Micromachined Gyroscopes in the Presence of Imperfections," *Proc. of the Int. Conf. Modeling and Simulation of Microsystems*, April 1999, pp. 605-608.

[13] A. M. Shkel, R. Horowitz, A. A. Seshia, S. Park, and R. T. Howe, "Dynamics and Control of Micromachined Gyroscopes," *Proc. of the American Control Conference*, San Diego, CA, June 1999, vol. 3, pp. 2119-2124.

[14] T. K. Tang, R. C. Gutierrez, C. B. Stell, V. Vorperian, G. A. Arakaki, J. T. Rice, W. J. Li, I. Chakraborty, K. Shcheglov, J. Z. Wilcox, and W. J. Kaiser, "A Packaged Silicon MEMS Vibratory Gyroscope for Microspacecraft," *Proc. IEEE of 10th Ann. Int. Workshop on MEMS*, Nagoya, Japan, Jan 1997, pp. 500-505.

[15] T. K. Tang, R. C. Gutierrez, J. Z. Wilcox, C. Stell, V. Vorperian, M. Dickerson, B. Goldstein, J. L. Savino, W. J. Li; R. J. Calvet, I. Charkaborty, R. K. Bartman, and W. J. Kaiser, "Silicon Bulk Micromachined Vibratory Gyroscope for Microspacecraft," *Proc. SPIE of Int. Soc. of Optical Engineering*, 1996, vol. 2810, pp. 101-115.

[16] N. Yazdi, F. Ayazi, and K. Najafi, "Micromachined Inertial Sensors," *Proc. IEEE*, Aug 1986, vol. 86, no. 8, pp. 1640-1659.